

Predicting the Future Performance of the Planned Seismic Network in Mainland China: II. Earthquake Early Warning

Jiawei Li¹, Didier Sornette^{1,2}, and Yu Feng^{1,3}

¹ Institute of Risk Analysis, Prediction and Management (Risks-X), Academy for Advanced Interdisciplinary Studies, Southern University of Science and Technology (SUSTech), Shenzhen, China, 518055.

² Department of Management, Technology and Economics (D-MTEC), Swiss Federal Institute of Technology in Zürich (ETH Zürich), Zürich, Switzerland, 8092.

³ Department of Earth and Space Sciences, Southern University of Science and Technology (SUSTech), Shenzhen, China, 518055.

Abstract The China Earthquake Administration (CEA) has launched an ambitious nationwide earthquake early warning (EEW) system project that is currently under development, which will consist of approximately 15,000 seismic stations and be the largest EEW system in the world. The new EEW system is planned to go online by the end of 2022. In 23% and 3% of Mainland China, the inter-station distance will soon be smaller than 50 km and 25 km, respectively. The effectiveness of the EEW system expected inside Mainland China can be quantified via the metric given by the radius of the blind zone (no-warning zone). Using theoretical network-based method, we generate the spatial distribution of the blind zone radii predicted for the new seismic network based on its configuration. The densified new seismic network is expected to have excellent EEW performance from the perspective of blind zone. The area covered by blind zones that are smaller than 30 km will soon rise from 1.6% to 24.3% inside Mainland China, which means that the area will increase by 2.6 million km² (almost the size of Kazakhstan). We claim that every 1,000,000 RMB (158,000 USD) invested to densifying the planned network will increase the area where the blind zone radius is smaller than 30 km by 3,000 km². Continuing to increase the density of stations in some key regions with the blind zone radii ranging from 20 to 40 km is still necessary to control the

unexpected expansion of blind zones due to the possible (and common) stations failure. Our investigation provides a useful reference for the real functioning and further optimization of the EEW system in Mainland China.

Keywords seismic network assessment; earthquake early warning (EEW); blind zone; system latency; earthquake risk mitigation; Mainland China.

1. Introduction

The densification of a seismic network reduces blind zones (or no-warning zones) of earthquake early warning (EEW) system (Kuyuk & Allen, 2013). The reduction of blind zones improves real-time EEW effectiveness by providing more positive lead time (or available warning time) and thus better mitigates earthquake risks (Pan et al., 2019; Wu et al., 2019; Cremen et al., 2022). System latency has been considered to be the reason for the existence of blind zone for shallow earthquakes and is determined by many factors, e.g., network density, speed of data transmission and system processing (Kuyuk & Allen, 2013; Chen et al., 2015; Picozzi et al., 2015; Guo et al., 2016; Li & Wu, 2016; Festa et al., 2018). Li et al. (2021) proposed the following empirical relationship based on a playback investigation of 58 earthquakes ($5.0 \leq M \leq 8.0$) in the Sichuan-Yunnan region, China, for a line-source model-based EEW algorithm:

$$T_{\text{tri}} = 2.5 \exp(0.04 D_{\text{epi}}) \quad (1)$$

where T_{tri} is the time when the algorithm triggers, counted from the origin time of the earthquake with an inter-station distance D_{epi} at its epicenter. The inter-station distance at a given site is defined as the average distance from this site to its closest fourth stations (Kuyuk & Allen, 2013). T_{tri} can be converted into the radius of the blind zone by a simple multiplication by the S -wave velocity. The radius of the blind zone is the simplest and one of the best proxies of the performance of an EEW system. Although it is impossible to declare an alert within a blind zone, the EEW system can be still useful for the sites outside the blind zone near the fault rupture, which is especially relevant for earthquakes with hundred kilometers ruptures (Böse et al., 2012; 2015; 2018; 2021; Ma et al., 2012; Li et al., 2018; 2020). It is a geometric fact that a blind zone with a radius of 10 km to 20 km is inevitable for

a shallow earthquake, no matter how dense is the network (Kuyuk & Allen, 2013; Wald, 2020). Optimization of an EEW system requires minimizing the blind zone size.

Inspiring by the developments of the EEW systems, and also the benefit from them, in the other regions worldwide (Allen et al., 2009; Satriano et al., 2011a; Strauss & Allen, 2016; Allen & Melgar, 2019; Allen & Stogaitis, 2022), Mainland China has been continuously developing and evolving EEW systems at city/infrastructure and regional/provincial scales in order to improve their capability for earthquake risk mitigation in the past three decades (e.g., Li et al., 2004; Peng et al., 2011; Li, 2014; Zhang et al., 2016; Peng et al., 2020; 2021). To extend the scale and applications of the existing seismic network, the National System for Fast Report of Intensities and Earthquake Early Warning Project of China launched by the China Earthquake Administration (CEA) has started a nationwide network construction project with a total investment of approximately 1.87 billion RMB (290 million USD; <https://www.cenc.ac.cn/cenc/zt/361404/361414/361563/index.html>, last accessed: January 2022). Through this project, the number of seismic stations will increase from approximately 2,000 to 15,000 in the near future, with the data planned to be transmitted with very little latency (Jiang & Liu, 2016). Pan et al. (2019) predicted the system latencies of the existing prototype and planned EEW systems of Gansu province in China based on their configurations and concluded that the performance of the planned EEW system will be significantly improved. The network-based method for calculating the radii of blind zones proposed by Kuyuk and Allen (2013) can be used to predict the spatial distribution of blind zones for the planned EEW system with the advantages of fewer assumptions compared with Pan et al. (2019).

Unlike the real single case-based analysis (e.g., Satriano et al., 2011b; Pazos et al., 2015; Li et al., 2018; Hsu et al., 2018), the theoretical network-based method requires several hypotheses (Kuyuk & Allen, 2013; Li & Wu, 2016). The minimum number of trigger stations is a critical one among them. The majority of the EEW systems worldwide adopt two to four stations as the minimum number to trigger. However, due to stations near the epicenter failing to work (Bormann, 2002) or underestimating ground-shaking hazards (Ma et al., 2012) in the real

world, the EEW system has to require a larger number of stations to trigger, which implies increasing the average inter-station distance and therefore expanding the blind zone. Consequently, Li and Wu (2016) proposed that there is a possible "soft" blind zone around the original ("hard") blind zone when taking account of the potential stations failure, and argued that the "soft" blind zone could be easily controlled by simply densifying the seismic network. Although an unexpected expansion of the blind zone ("soft" blind zone) is common and challenges the success of an EEW system, there is no study that quantitatively investigates how the EEW effectiveness is affected by the "soft" blind zone, so far.

In this study, we predict the EEW performance estimated by the radii of blind zones for the planned seismic network. We begin with a brief introduction to the new EEW system in Mainland China. Then, we predict the improvement of the planned network compared with the existing network from the perspective of the spatial distribution of blind zones. Finally, the significance of controlling the "soft" blind zones is discussed quantitatively. Our work will help to guide the design and optimization of the planned EEW system in Mainland China.

2. Data

The new seismic network in Mainland China consists of a total of approximately 15,000 stations: approximately 2,000 datum stations equipped with broadband seismometers and accelerometers, approximately 3,200 basic stations equipped with only accelerometers, and approximately 10,000 ordinary stations equipped with low-cost micro-electro-mechanical system (MEMS) intensity sensors (Table 1). In 23% and 3% of Mainland China, the inter-station distance will soon be smaller than 50 km and 25 km, respectively. The new network is expected officially be online by the end of 2022 (Wenhui Huang, written comm., 2021). The new network will be the main backbone of the largest EEW system in the world. In the future, EEW services will be provided in five key regions (North China, the central China north-south seismic belt, the southeast coast, the middle section of the Tianshan Mountains in Xinjiang, and Lhasa in Tibet; Figure 1). The seismic intensity will be reported

rapidly within minutes from the origin time for the whole Mainland China, and the monitoring capability in Mainland China will be significantly improved (Li et al., 2022). To compare with the planned EEW system, we also envisage a virtual EEW system by combining the existing high-gain broadband seismic and strong motion networks with a total of approximately 950 and 1,100 stations, respectively. For the description of the distributions of stations and inter-station distance for the existing and planned networks, we refer to the Supplement Information of Li et al. (2022).

Table 1. Costs of the new stations in the planned seismic network in Mainland China.

Items	DT station	BS station	OD station
The site construction	90,000	60,000	N/A
The data acquisition system	50,000	40,000	N/A
A broadband seismometer	60,000	N/A	N/A
An accelerometer	15,000	15,000	N/A
A MEMS sensor	N/A	N/A	10,000
other accessories	20,000	15,000	N/A
Total	235,000	130,000	10,000

DT station: datum station; BS station: basic station; OD station: ordinary station; BB station: broadband seismic station; SM station: strong motion station. Costs are YUAN in RMB. Data from Qiang Ma and Changsheng Jiang (written comm., 2021).

3. Earthquake early warning performance estimated by blind-zone

Considering that most ordinary stations equipped with MEMS sensors are with relatively low observational quality to detect the early part of waveforms, we choose conservatively for this study a minimum number of three trigger stations. Hypothesizing an homogeneous Earth crust model, the P -wave travel time at the third closest station with epicenter distance Δ from a point source with depth H is given by:

$$t_P = \frac{\sqrt{\Delta^2 + H^2}}{V_P} \quad (2)$$

Then, with the system latency T for processing and data transmission, the horizontal distance r_{BZ} of S -wave propagation is

$$r_{BZ} = \sqrt{(t_P + T)^2 V_S^2 - H^2} \quad (5)$$

This means that the S -wave has already arrived before the alarm is released at distances smaller than r_{BZ} from the earthquake epicenter. The disk with radius r_{BZ} is called the blind zone in the EEW system.

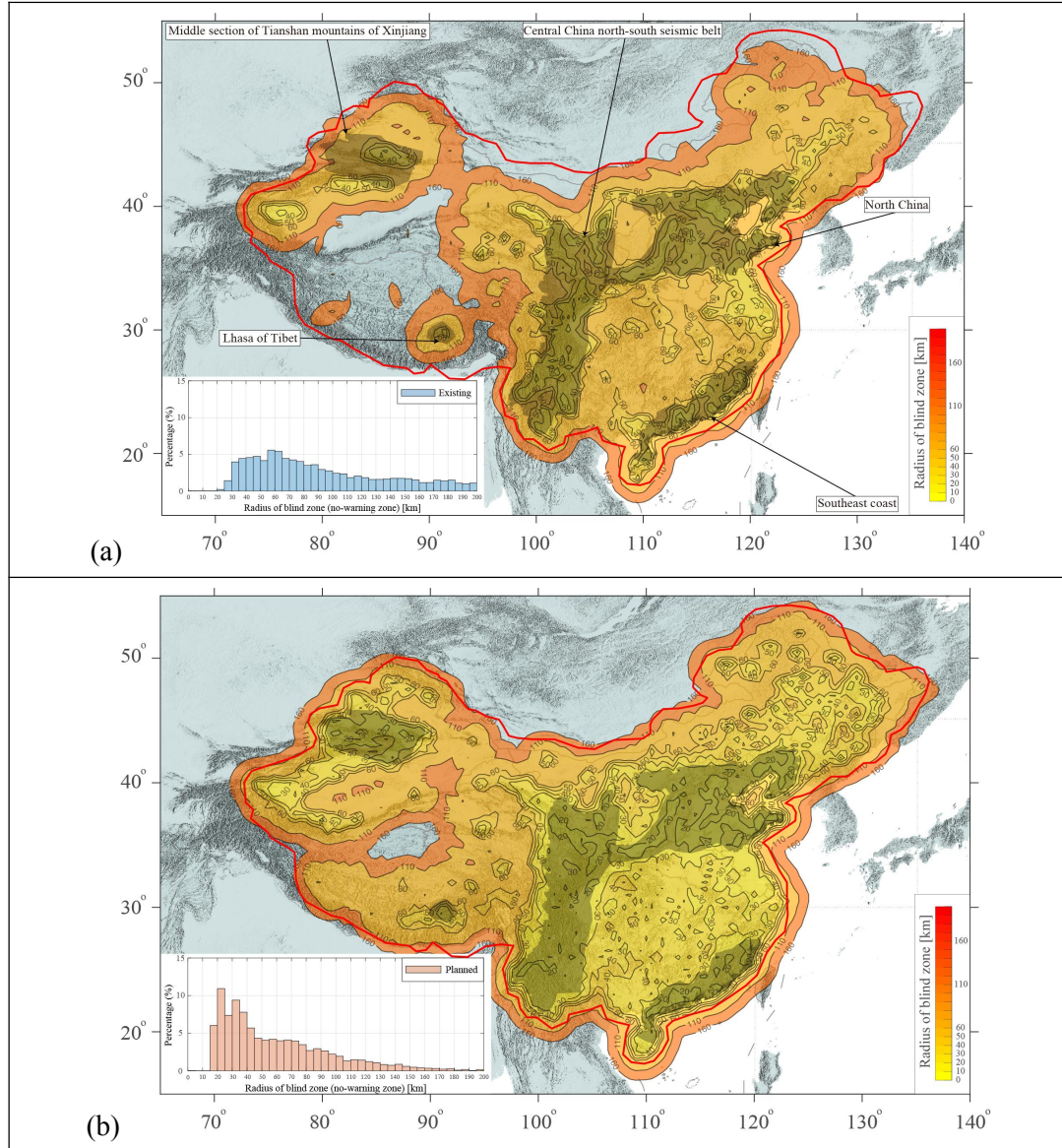


Figure 1. Maps showing the estimated radii of blind zones (no-warning zones) for the (a) existing and (b) planned networks assuming a minimum number of three trigger stations and system latencies of 5 s and 4 s, respectively. The average focal depth and P - and S -wave velocities for the calculation are assumed to be 5 km, 6 km/s, and 3.5 km/s, respectively. Red lines show the region within 100 km outside of Mainland China’s boundaries, which is defined as “inside” in this study. The histograms in the bottom left show the binned distributions of the radii of blind zones inside Mainland China. The dark areas are the five key earthquake early warning (EEW) regions that will be in operation after 2022.

For the purpose of this study, we define the inside of Mainland China as the region within 100 km outside of the boundaries of Mainland China and Hainan Island (approximately 11.5 million km²; Red lines in Figure 1). Figures 1a and 1b show the size distribution of blind zones assuming $H = 5$ km, $V_P = 6$ km/s, and $V_S = 3.5$ km/s, processing time of 3 s and data transmission latencies of 1 s and 2 s for the planned and existing networks (Wenhui Huang, written comm., 2021) using a mesh of $0.5^\circ \times 0.5^\circ$ resolution. The regions (accounting for approximately 1.6% of the area inside Mainland China) with existing blind zones that are smaller than 30 km are distributed only around several large cities (e.g., Beijing-Tianjin, Guangzhou-Shenzhen), while they increase to 24.3% for the planned network and include the majority of North China, Southeast China, the central China north-south seismic belt, and Xinjiang. The binned distributions of blind zone radii (Figure 1a and 1b) show that approximately 42% of the region inside Mainland China will have a blind zone radius smaller than 40 km. In 6.0% of Mainland China, the blind zone radii of the planned network are smaller than 20 km, which is of great significance for the successful functioning of the EEW system.

4. “Soft” blind zone and its control

Based on a series of evenly distributed modeled shallow point-sources and stations, Kuyuk and Allen (2013) determined a semiquantitative empirical curve that describes the relationship between the minimum number of trigger stations, the inter-station distance and the blind zone radius (Figure 2a). The main feature shown in Figure 2a ($D_1 < D_2$; $r_{BZ1} < r_{BZ2}$) is that the blind zone radius decreases dramatically with the decrease of inter-station distances when the network density of seismic stations is small. While for a very dense network, the blind zone radius converges to a plateau (10 to 20 km depending on different conditions), which is approximately the same for different minimum number of trigger stations.

Figure 2a can also be used to illustrate an equivalence principle between the minimum number of trigger stations and network density from the perspective of blind zones. Assuming a seismic network with inter-station distance D_1 , the minimum number of N trigger stations

corresponds to a blind zone of radius r_{BZ1} (point A in Figure 2a). Li et al. (2016) called this ideal blind zone with radius r_{BZ1} the theoretical "hard" blind zone. In the real world, some i stations near the epicenter may fail to work properly (Bormann, 2002) or to be triggered due to an underestimation of ground-shaking (e.g., YZP station during the 2008 M_S 8.0 Wenchuan earthquake; Ma et al., 2012). Therefore, the EEW system has to adopt i more stations to be triggered, which corresponds to point B with a blind zone radius r_{BZ2} ($r_{BZ1} < r_{BZ2}$) in Figure 2a. This unexpected and larger blind zone with radius r_{BZ2} is called the "soft" blind zone by Li et al. (2016). From Figure 2a, the size of this "soft" blind zone is equivalent to the size of the "hard" blind zone of a seismic network adopting a minimum number N of trigger stations with inter-station distance D_2 ($D_1 < D_2$) in point C.

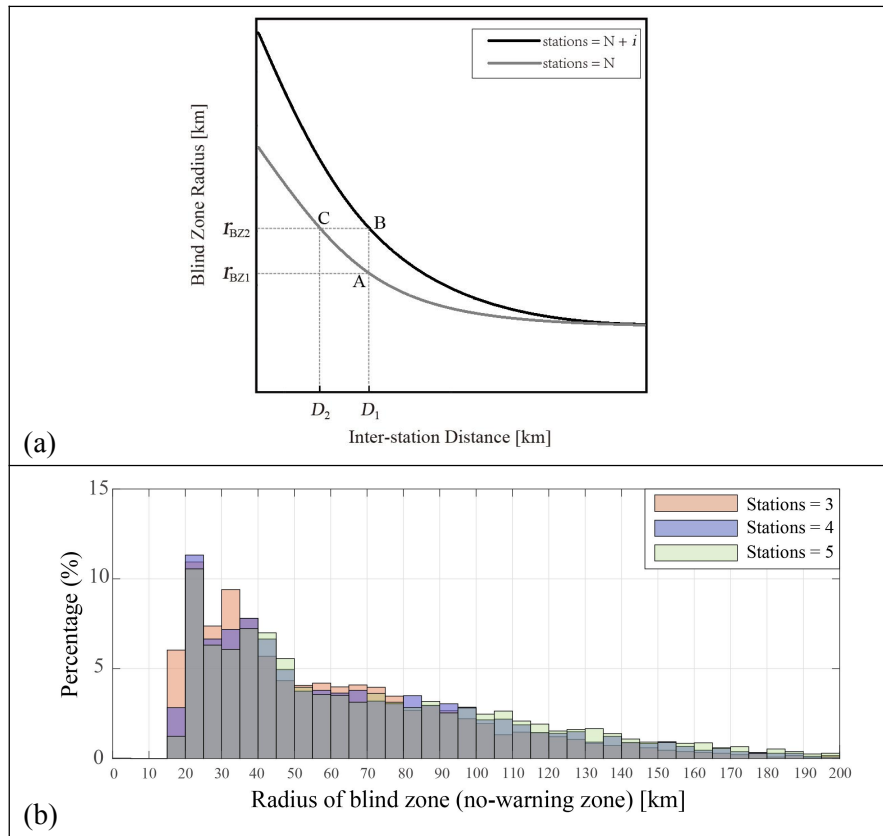


Figure 2. (a) The relationship between the blind zone radius and the inter-station distance for different numbers of trigger stations. The x-axis decreases from left to right ($D_1 < D_2$) corresponding to an increasing network density, and the y-axis increases from bottom to top ($r_{BZ1} < r_{BZ2}$). Modified from Figure 5 of Kuyuk and Allen (2013). (b) The binned distribution of the blind zone radii inside Mainland China for the case of three, four, and five trigger stations, respectively. The binned distribution for the case of three trigger stations is same as that in the bottom left of Figure 1b.

To investigate the performance of the planned EEW system of China (assuming $N = 3$, same as [Figure 1](#)) affected by the "soft" blind zone, we show the binned distribution of blind zones inside Mainland China for $i = 1$ and $i = 2$ potential station failures, respectively ([Figure 2b](#)). The areas with r_{BZ} smaller than 20 km, 30 km, and 40 km account for 2.8%, 20.8%, and 38.8% of the total area for $N + i = 4$, and for 1.2%, 18.1%, and 35% for $N + i = 5$, respectively. Compared with [Figure 1b](#) ($N = 3$), the area with r_{BZ} smaller than 20 km is reduced by factors of 1 and 5 for $N + i = 4$ and 5, respectively. The proportion of areas with r_{BZ} smaller than 30 km and 40 km decreases by 3.5 to 4.0 percentage points for $N + i = 4$, and 6.0 to 8.0 percentage points for $N + i = 5$. Overall, continuing to densify the seismic network in some regions where r_{BZ} ranges from 20 to 40 km is still recommended to control the "soft" blind zones and minimize blind zones.

5. Discussion

The above theoretical conclusions about blind zones predicted for the planned network can be validated by blind zones estimated by the empirical Equation (1) multiplied by $V_s = 3.5$ km/s. This equation is regressed with the Finite-Fault Rupture Detector (FinDer) algorithm ([Böse et al., 2012; 2015; 2018](#)), with a trigger threshold of 4.6 cm/s^2 , a minimum number of three trigger stations, and assuming no data transmission latency ([Li et al., 2021](#)). Previous studies have shown that the T_{tri} values of other point-source-based algorithms are slightly different from those of the FinDer algorithm (e.g., [Li et al., 2020; Kohler et al., 2020](#)). Therefore, we propose that Equation (1) regressed by [Li et al. \(2021\)](#) can be adopted into the EEW systems with the same trigger configurations to estimate the system latency with uncertainty ($\sigma = 1.8$ s). [Figure 3](#) shows that the area with empirical r_{BZ} smaller than 40 km account for 41.9%, close to the theoretical r_{BZ} result (42.6%) in [Figure 1b](#). However, the empirical r_{BZ} for 20 and 30 km are 8.0 to 10.0 percentage points larger than the theoretical results. We explain this as due to higher uncertainties of the empirical Equation (1) for the smaller inter-station distances.

The costs per station of 1,000 new datum, 2,100 new basic, and 10,000 new ordinary stations

of the planned network are 235,000 RMB, 130,000 RMB, and 10,000 RMB, respectively (Table 1; Qiang Ma and Changsheng Jiang, written comm., 2021). Compared with the cost of building existing broadband seismic (350,000 RMB) and strong motion (200,000 RMB) stations in 2008 (Table 1; Qiang Ma and Changsheng Jiang, written comm., 2021), the station construction cost decreased, which was mainly due to the localized development and production of seismometers and the decline in their prices. The upgrade (to replace the data acquisition system and seismometer) costs per station of 1,000 existing broadband seismic and 1,100 strong motion stations are 125,000 RMB and 55,000 RMB, respectively. Therefore, the cost directly used to increase the density of the stations is 794 million RMB, accounting for approximately 42% of the total investment (1.87 billion RMB).

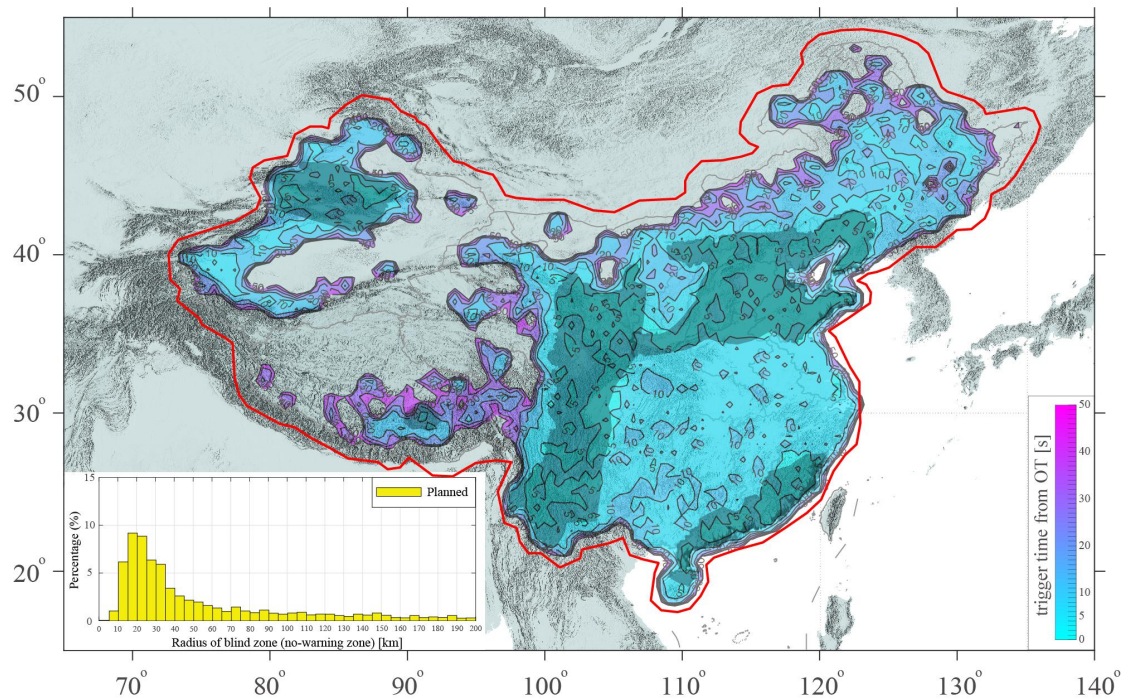


Figure 3. Maps showing the estimated EEW system trigger time T_{tri} from the earthquake origin time for the planned network assuming data transmission latency of 1 s. The areas colored in cyan have the fastest system trigger. The histogram in the bottom left shows the binned distribution of the blind zone radii inside Mainland China obtained from Equation (1) by multiplying it by $V_s = 3.5$ km/s. Same as Figure 1.

Figure 1 shows that the area covered by blind zones that are smaller than 30 km will increase from 1.6% to 24.3% inside Mainland China (11.5 million km^2), which means that this area will increase by 2.6 million km^2 (almost the size of Kazakhstan). Assuming the improvement

is made through the densification of the seismic network with an investment of 794 million RMB, we claim that every 1,000,000 RMB (158,000 USD) invested in the planned networks will increase the area where the blind zone radius is smaller than 30 km by 3,000 km².

6. Conclusions

The performance of an EEW system will significantly improve by simply densifying the existing layout. In 23% and 3% of Mainland China, the inter-station distance will be smaller than 50 km and 25 km by the end of 2022. In this study, we predicted the spatial distribution of the blind zone radii and quantified the warning effectiveness of the planned EEW system in Mainland China based on its network configuration. The area covered by blind zones that are smaller than 30 km will increase from 1.6% to 24.3% inside Mainland China, which means that this area will increase by 2.6 million km² (almost the size of Kazakhstan). This is of great significance for the successful functioning of the nationwide EEW system. Assuming the improvement is made through the densification of the seismic network, we claimed that every 1,000,000 RMB (158,000 USD) invested in the planned networks will increase the area where the blind zone radius is smaller than 30 km by 3,000 km². Taking into account that stations near the epicenter may fail to work properly or may underestimate ground-shaking hazards, the proportion of areas with r_{BZ} smaller than 30 km and 40 km decreases by 3.5 to 4.0 percentage points for one station failure, and by 6.0 to 8.0 percentage points for two station failures. To control the unexpected expansion of blind zones due to common station failures, it is still necessary to continue to densify the seismic network in some key regions with the blind zone radii ranging from 20 to 40 km. Our investigation provides a useful reference for the real functioning and further optimization of the EEW system in Mainland China.

Acknowledgments

The authors would like to thank Prof. Zhongliang Wu at the Institute of Earthquake Forecasting of China Earthquake Administration (CEA) for discussion about blind zone, Dr. Chen Yang and Dr. Yang Zang at the China Earthquake Networks Center for providing

information on the stations. This project is supported by the National Natural Science Foundation of China under Grant No. U2039202 and the Guangdong Basic and Applied Basic Research Foundation under Grant No. 2020A1515110844.

Conflict of Interest

The authors declare that they have no conflict of interest.

References

- Allen R M, Gasparini P, Kamigaichi O, Bose M. 2009. The status of earthquake early warning around the world: An introductory overview. *Seismol Res Lett*, 80: 682-693.
- Allen R M, Melgar D. 2019. Earthquake early warning: Advances, scientific challenges, and societal needs. *Ann Rev Earth Planet Sci*, 47: 361-388.
- Allen R M, Stogaitis M. 2022. Global growth of earthquake early warning. *Science*, 375: 717-718.
- Bormann P. 2002. New manual of seismological observatory practice. GeoForschungsZentrum, Potsdam.
- Böse M, Heaton T H, Hauksson E. 2012. Real-time finite fault rupture detector (FinDer) for large earthquakes. *Geophys J Int*, 191: 803-812.
- Böse M, Felizardo C, Heaton T H. 2015. Finite-fault rupture detector (FinDer): Going real-time in Californian ShakeAlert warning system. *Seismol Res Lett*, 86: 1692-1704.
- Böse M, Smith D E, Felizardo C, Meier M A, Heaton T H, Clinton J F. 2018. FinDer v.2: Improved real-time ground-motion predictions for $M2-M9$ with seismic finite-source characterization. *Geophys J Int*, 212: 725-742.
- Böse M, Hutchison A A, Manighetti I, Li J W, Massin F, Clinton J F. 2021. FinDerS (+)-Real-time slip profiles and magnitudes estimated from backprojected Seismic and geodetic displacement amplitudes. *Front Earth Sci*, 9, 685879.
- Chen Y, Guo K, Zhang S L, Huang Z B. 2015. Status quo of China earthquake networks and analyses on its early warning capacity (in Chinese with English abstract). *Acta Seismologica Sinica*, 37: 508-515.

- Cremen G, Galasso C, Zuccolo E. 2022. Investigating the potential effectiveness of earthquake early warning across Europe. *Nat Comm*, 13: 639.
- Festa G, Picozzi M, Caruso A, Colombelli S, Cattaneo M, Chiaraluce L, Elia L, Martino C, Marzorati S, Supino M, Zollo, A. 2018. Performance of earthquake early warning systems during the 2016-2017 M_w 5-6.5 Central Italy sequence. *Seismol Res Lett*, 89: 1-12.
- Guo K, Wen R Z, Yang D K, Peng K Y. 2016. Effectiveness evaluation and social benefits analyses on earthquake early warning system (in Chinese with English abstract). *Acta Seismologica Sinica*, 38: 146-154.
- Hsu T Y, Lin P Y, Wang H H, Chiang H W, Chang Y W, Kuo C H, Lin C M, Wen K L. 2018. Comparing the performance of the NEEWS earthquake early warning system against the CWB system during the 6 February 2018 M_w 6.2 Hualien earthquake. *Geophys Res Lett*, 45: 6001-6007.
- Jiang C S, Liu R F. 2016. National Seismic Intensity Rapid Reporting and Early Warning Project: Opportunity and challenge of seismic network (in Chinese with English abstract). *Journal of Engineering Studies*, 3: 250-257.
- Kohler M D, Smith D E, Andrews J, Chung A I, Hartog R, Henson I, Given D D, de Groot R, Guiwits S. 2020. Earthquake early warning ShakeAlert 2.0: Public rollout. *Seismol Res Lett*, 91: 1763-1775.
- Kuyuk H S, Allen R M. 2013. Optimal seismic network density for earthquake early warning: A case study from California. *Seismol Res Lett*, 84: 946-954.
- Li X. 2014. Study on earthquake intensity rapid report system in Wuhan city circle (in Chinese with English abstract). (Beijing: Institute of Geophysics, China Earthquake Administration). [dissertation/doctoral thesis].
- Li S Y, Jin X, Ma Q, Song J D. 2004. Study on earthquake early warning system and intelligent emergency controlling system (in Chinese with English Abstract). *World Earthquake Eng*, 20: 21-26.
- Li J W, Wu Z L. 2016. Controlling the 'blind zone' of an earthquake early warning system (EEWS): A case study of the Beijing Capital Circle prototype EEWS (in Chinese with English abstract). *Earthq Res China*, 32: 584-594.

- Li J W, Zhang S F, Zhang Y. 2018. Seismic finite source and its significance to earthquake early warning system (EEWS) (in Chinese with English abstract). *Acta Seismologica Sinica*, 40: 728-736.
- Li J W, Böse M, Wyss M, Wald D J, Hutchison A, Clinton J F, Wu Z L, Jiang C S, Zhou S Y. 2020. Estimating rupture dimensions of three major earthquakes in Sichuan, China, for early warning and rapid loss estimates. *Bull Seismol Soc Am*, 110: 920-936.
- Li J W, Böse M, Feng Y, Yang C. 2021. Real-time characterization of finite rupture and its implication for earthquake early warning: Application of FinDer to existing and planned stations in Southwest China. *Front Earth Sci*, 9: 699560.
- Li J W, Mignan A, Sornette D, Feng Y. 2022. Predicting the future performance of the planned seismic network in Mainland China. *Geophys Res Lett* (under review).
- Ma X J, Wu Z L, Peng H S, Ma T F. 2012. Challenging the limit of EEW: A scenario of EEWS application based on the lessons of the 2008 Wenchuan earthquake. In *Advances in Geosciences*, Vol 31, Lo C H. (eds) World Scientific, New Jersey, 11-22.
- Pan Z, Tian X, Zhang W, Yuan J. 2019. Analysis on early warning capability of Gansu earthquake early warning stations network. *IOP Conf Ser Earth Environ Sci*, 304: 042027.
- Pazos A, Romeu N, Lozano L, Colom Y, López Mesa M, Goula X, Jara J A, Cantavella J V, Zollo A, Hanka W, Carrilho F. 2015. A regional approach for earthquake early warning in south west Iberia: A feasibility study. *Bull Seismol Soc Am*, 105: 560-567.
- Peng C Y, Ma Q, Jiang P, Huang W H, Yang D K, Peng H S, Chen L, Yang J S. 2020. Performance of a hybrid demonstration earthquake early warning system in the Sichuan-Yunnan border region. *Seismol Res Lett*, 91: 835-846.
- Peng C Y, Jiang P, Ma Q, Wu P, Su J R, Zheng Y, Yang J S. 2021. Performance evaluation of an earthquake early warning system in the 2019–2020 $M6.0$ Changning, Sichuan, China, seismic sequence. *Front Earth Sci*, 9: 699941.
- Peng H S, Wu Z L, Wu Y M, Yu S M, Zhang D N, Huang W H. 2011. Developing a prototype earthquake early warning system in the Beijing Capital Region. *Seismol Res Lett*, 82: 394-403.
- Picozzi M, Zollo A, Brondi P, Colombelli S, Elia L, Martino C. 2015. Exploring the

feasibility of a nationwide earthquake early warning system in Italy. *J Geophys Res*, 120: 2446-2465.

Satriano C, Wu Y M, Zollo A, Kanamori H. 2011a. Earthquake early warning: Concepts, methods and physical grounds. *Soil Dyn Earthq Eng*, 31: 106-118.

Satriano C, Elia L, Martino C, Lancieri M, Zollo A, Iannaccone G. 2011b. PRESTo, the earthquake early warning system for southern Italy: Concepts, capabilities and future perspectives. *Soil Dyn Earthq Eng*, 31: 137-153.

Strauss J A, Allen R M. 2016. Benefits and costs of earthquake early warning. *Seismol Res Lett*, 87: 765-772.

Wald D J. 2020. Practical limitations of earthquake early warning. *Earthq Spectra*, 36: 1412-1447.

Wu Y M, Mittal H, Huang T C, Yang B M, Jan J C, Chen S K. 2019. Performance of a low-cost earthquake early warning system (P-Alert) and shake map production during the 2018 M_w 6.4 Hualien, Taiwan, earthquake. *Seismol Res Lett*, 90: 19-29.

Zhang H C, Jin X, Wei Y X, Li J, Kang L C, Wang S C, Huang L Z, Yu P Q. 2016. An earthquake early warning system in Fujian, China. *Bull Seismol Soc Am*, 106: 755-765.